First Application of a Theoretically Derived Coupling Function in Cosmic Ray Intensity for the case of the September 10, 2017 Ground Level Enhancement GLE 72

L. Xaplanteris[1,*], M. Gerontidou[1] , H. Mavromichalaki[1], J. V. Rodriguez[5,6], M. Livada[1], M. K. Georgoulis[3], T. E. Sarris[4], V. Spanos[1], L. Dorman[2]

[1] Nuclear and particle Physics Department, Faculty of Physics, National and Kapodistrian University of Athens, Zografos, 15784 Athens, Greece
[2] Israel Cosmic Ray and Space Weather Center and Emilio Serge Observatory, Tel Aviv University, Golan Research Institute and Israel Space Agency, Israel
[3] Research Center of Astronomy and Applied Mathematics, Academy of Athens, Athens Greece
[4] Department of Electrical and Computer Engineering, Democritus University of Thrace, Xanthi, Greece
[5] Cooperative Institutes for Research in Environmental Sciences, University of Colorado, Boulder, Colorado, USA
[6]NOAA National Centers for Environmental Information, Boulder, Colorado, USA

*Corresponding author: Loukas Xaplanteris email: ksaplant@phys.uoa.gr

Abstract
In this work we implement an analytically derived coupling function between ground level and primary proton particles for the case of Ground Level Enhancement events (GLEs). The main incentive for this work is to determine whether this coupling function is suitable for the study of both major cases of Cosmic Rays (CRs) variation events, namely GLEs and Forbush decreases. This version of the coupling function, which relies on formalism used in Quantum Field Theory (QFT) computations, has already been applied to Forbush decreases yielding satisfactory results. In this study, it is applied to a GLE event that occurred on September 10, 2017. For the analytical derivations, normalized ground level cosmic ray data were used from seven Neutron Monitor stations with low cutoff rigidities. To assess and evaluate the results for the normalized proton intensity, we benchmark them with the time series for the proton flux, as recorded by the GOES 13 satellite during the same time period. The theoretically calculated results for proton energy ≥ 1 GeV are in general agreement with the recorded data for protons with energy > 700 MeV, presenting a least-squares linear best fit with slope 0.75 ± 0.17 and a Pearson correlation coefficient equal to 0.62. We conclude that the coupling function presented in this work is the first coupling function that is well applicable to both cases of cosmic ray intensity events, namely GLEs and Forbush decreases.

Keywords: Neutron Monitors, Cosmic Rays, Coupling functions, Ground Level Enhancements

1. Introduction

Cosmic Rays (CRs) are highly energetic particles originating from various sources within or beyond our solar system – and even galaxy – that are constantly present at Earth and its space surroundings. Galactic Cosmic Ray (GCR) flux consists mostly of protons and is modulated heavily by solar activity in the course of the nominal, 11-year Solar Cycle (SC).

Apart from GCRs, at times, high-energy particles of solar origin also appear; they are commonly referred to as solar energetic particles (SEPs), and are produced during powerful solar eruptions, such as major solar eruptive flares associated with coronal mass ejections (CMEs). SEP events of exceptional intensity and energy (i.e., above 400-500 MeV) manage to precipitate through Earth's magnetosphere and atmosphere. During their atmospheric propagation, they participate in multiple collisions/interactions with (neutral) atmospheric particles, producing atmospheric showers of secondary particles, some of which are recorded by ground-based detectors, such as neutron monitors (NMs) (Simpson, 2000). These classes of highly energetic SEP events that are recorded on the ground are known as Ground Level Enhancements (GLEs) and were identified initially by Forbush (1946). GLE events are of great importance mainly because their study can reveal important information on particle acceleration mechanisms in interplanetary space as well as the structure and properties of the interplanetary magnetic field (Dorman, 2004; Andriopoulou et al., 2011; Balabin et al., 2018). In addition, GLE events have a significant effect on the short-time variation of atmospheric ionization (Velinov et al., 2013). Recently, it was found that an extreme SEP event could even lead to a large increase in fair-weather downward current density on a global scale (Golubenko et al., 2020). Moreover, the study of GLEs is deemed very important for the determination of radiation dosage at airplane altitudes (Bütikofer and Flückiger, 2009; Mishev et al., 2018; Copeland, Matthiä and Meier, 2018; Mishev and Usoskin, 2018; Kataoka, 2018; Tezari et al., 2020) and for understanding the effects of particulate radiation on human health in general (Shea et al., 2000). GLEs are most commonly recorded by high latitude NM stations where the geomagnetic field lines are significantly more "open", i.e., closing at infinity. Given their relation to major solar eruptions, GLEs occur statistically during maxima of solar activity cycles.

September 2017 was the most active month in SC24, showing increased particle flux associated with solar activity. During the first ten days of the month, 19 GOES M-class and 4 GOES X-class solar flares were recorded. The two largest solar flares of this cycle, namely an X9.3 flare on September 6 and an X8.2 flare on September 10, were recorded only a few days apart. The X8.2 flare on September 10, 2017 was triggered at 15:35 UT at coordinates S08W88, within Active Region NOAA AR 12673 (hereafter AR12673). The flare reached its maximum at 16:06 UT, leading to high-energy SEP events with proton energies exceeding 700 MeV/nucleon. As measured by the SOHO/LASCO coronagraph, the initial speed of the CME was recorded at 3620 km/s, measured at angle 270^{o} to the west from the leading edge of the structure (Mishev et al., 2018). The result of this ultrafast CME and associated SEP events was the formation of GLE72, the first one since May 2012 and the second one of the

entire SC24. We note that during previous SC19 – SC23, the average occurrence of GLE events was one per year. Thus, SC24 is considered as a low activity cycle in terms of GLE events occurrence. The GLE72 event can be described as highly anisotropic and of low intensity (Kurt et al., 2019), as can be seen from the recorded GLE amplitudes of the NM stations (Table 1). According to the GLE Alert plus System of the National and Kapodistrian University of Athens (http://cosray.phys.uoa.gr/), the Fort Smith (FSMT) NM station was the first to record this event at 16:18 UT. After that, the Apatity (APTY) station at 16:47 UT, Kerguelen (KERG) at 16:53 UT and Inuvik (INVK) at 16:58 UT were in Alert Mode and an automated e-mail message was sent to registered users (Mavromichalaki et al., 2018).

In this work we apply the theoretically derived coupling function of Xaplanteris et al. (2020; 2021) to the GLE72 event. The main difference between our computed coupling function and others widely used is the methodology we applied, computing it analytically by means of fundamental Quantum Field Theory (QFT) calculations and tools (Feynman graphs, renormalization technique etc.) (Peskin, 1995; Weinberg, 1995; Griffiths, 2008; Srednicki, 2007). The majority of other coupling/yield functions are based on a statistical simulation model or tool. Examples of such coupling functions include:

- The Mishev et al. (2020) yield function, derived with the PLANETOCOSMICS simulation tool (Desorgher et al., 2005), based on the GEANT 4 package (Agostinelli et al., 2003).
- The Clem and Dorman (2000) function, derived numerically through Monte Carlo simulations.
- The Caballero-Lopez and Moraal function (2012), (Maurin et al., 2015) and its updated version Caballero-Lopez (2016), that considers muons, Cherenkov and stratospheric balloon detector response functions.

Our theoretically derived coupling function has already been tested on Forbush decreases (Fds), yielding satisfactory results. In particular, in its initial version it was used for the study of the Fds of February 2011 and March 2012, producing very encouraging results when compared to the ones obtained by Dorman's coupling function (Dorman, 2000; Xaplanteris et al., 2020), meaning very similar time profiles and amplitude values for the primary proton spectrum that differed less than 1%. Shortly thereafter, the improved version (wider energy spectrum and altitude correction factor) was applied to the Fd of September 2017 (and again March 2012), yielding again a high Pearson correlation coefficient of the order r=0.95 when compared to the coupling functions obtained by the Global Survey Method (GSM) (Belov et al., 2018; Xaplanteris et al., 2021).

The purpose of this work is to apply our coupling function to the case of GLE events, for the first time, in order to assess the suitability of this analytical approach for this important class of events, as well. We do not a priori see a theoretical reason why this function could not be used to describe GLE events, on top of Fd events. It is important to note that even though these two classes of events are of different nature, their observable effects on CR intensity are qualitatively similar: variations in

the form of normalized decrease or increase of the detected CR intensity. Our analytical model focuses solely on the computation of such variations, regardless of their origin. Moreover, a satisfactory application to GLE events would further increase the validity of the obtained results on the primary cosmic ray particles and render this approximation suitable for a wider range of CR events, meaning solar CR events such as study of solar winds, particle acceleration mechanisms and Space Weather applications.

2. Data Selection

2.1 Neutron Monitor data

For the study of GLE72, recorded on September 10, 2017 at 16:18 UT, 5-minute neutron monitor data corrected for pressure and efficiency were considered. The data were obtained from the high-resolution real time Neutron Monitor Database (NMDB, http://www.nmdb.eu) (Mavromichalaki et al., 2011). The choice of NM stations used in this study was based on the value of the cutoff rigidity of each station. More specifically, since GLE events become more evident in high latitude NM stations with low cutoff rigidity/ cutoff energy values and GLE72, in particular, was of low intensity (Kurt et al., 2019), we used data from seven NM stations with low cutoff rigidity values, ranging from 0.01 GV (TERA) to 1.65 GV (YKTK). Table 1 provides this information along with additional characteristics (abbreviation, geographic coordinates, atmospheric pressure at the time of detection, altitude, altitude correction factor, onset time and the recorded GLE amplitude).

NM Station	Abbrev.	Geogr. Coord.	Cutoff Rig. (GV)	Cutoff Energy (GeV)	Atm. Pressure (mb)	Altitude (m)	Alt. Cor. Factor	Onset Time (UT)	GLE Ampl. (%)
Yakutsk	YKTK	62.01 N 129.43 E	1.65	0.96	1003	105	1.02	16:30	6.26
Kerguelen	KERG	-49.35 S 70.27 E	1.14	0.53	1000	33	1.01	16:53	5.00
Apatity	APTY	67.57 N 33.4 E	0.65	0.20	1010	181	1.03	16:47	3.88
Oulu	OULU	65.05 N 25.47 E	0.80	0.30	1000	15	1.00	16:30	5.82
Fort Smith	FSMT	60.02 N 111.93 W	0.30	0.05	1000	180	1.03	16:18	6.07
Inuvik	INVK	68.36 N 122.72 W	0.30	0.05	1000	21	1.00	16:58	5.88
Terre Adelie	TERA	-66.7 W 140.0 E	0.01	0.00	987	32	1.00	17:01	6.37

Table 1: Characteristics of the neutron monitor stations considered for the study of GLE72 on September 10, 2017, including the recorded GLE amplitude of each station (the maximum % increase value).

Normally the inclusion of NM stations with cutoff energy values below 1 GeV (which corresponds to cutoff rigidity of 1.6 GV) would be avoided since our coupling function holds for energies above this value, E ≥ 1 GeV (Xaplanteris et al., 2021). That said, we consider the above stations in this study for two reasons: first, because the low-intensity GLE72 should be studied mostly by NM stations with lower cutoff rigidities in order to record significant event amplitudes. Second, because we seek to assess the applicability of our theoretical coupling function to NM stations with lower rigidities.

Time profiles of the normalized CR intensity from all seven NM stations used are shown in Figure 1. For the normalization of the intensity values, we used the known relation:

$$\frac{\delta N(t)}{N} = \frac{N(t) - N_0}{N_0} \quad (1)$$

where N_0 is the average intensity (counts/sec) for the 30 minutes preceding the start of the event (14:00-14:30, 5-min. values).

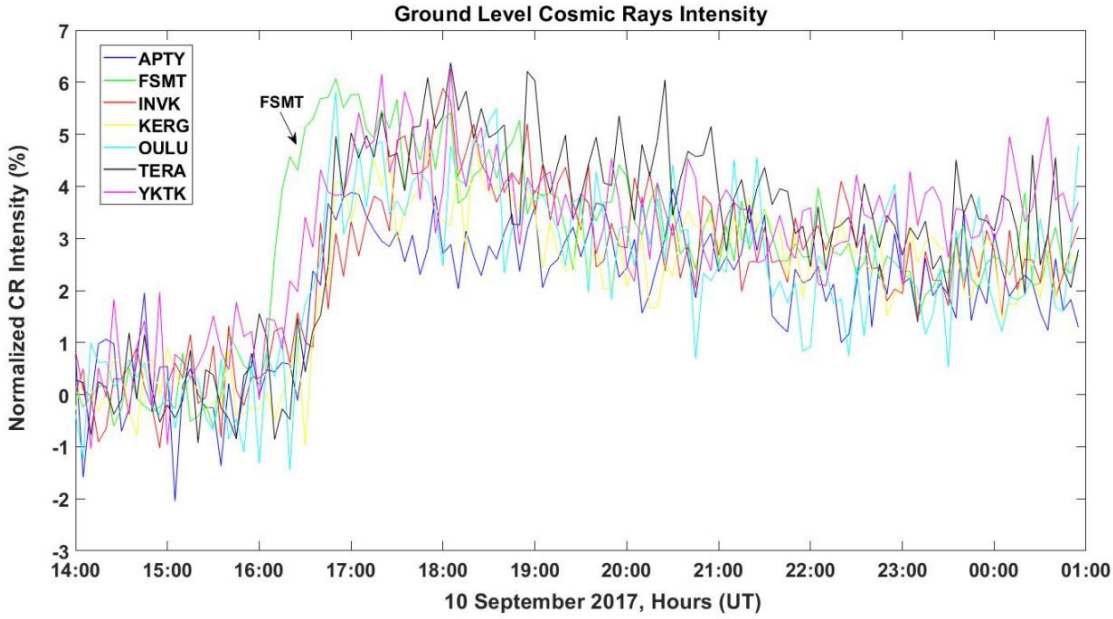

Fig. 1: Time profile of the normalized cosmic ray intensity recorded by seven NM stations on September 10, 2017, from 14:00 UT to 11 hours thereafter. The mean value of the interval 14:00-14:30 UT of this day was used for normalization. The early detection of the event by the Fort Smith NM (FSMT) station is indicated by an arrow.

In the computations, we used a power-law function for the proton normalized intensity (see Equation (5) below), as was done in the study of Fds by Xaplanteris et al. (2021). We note that the CR spectrum during GLE72 can be described by a combination of exponential and power-law forms (Balabin et al., 2018). Differences between the two kinds of spectra become evident in the high energy region. More specifically, if an exponential form is considered, then there are less high energy protons compared to the power-law form, due to the steeper depression of the spectrum slope. In GLE72, the proton spectrum was closer to a power-law form, meaning that more high-energy particles were present.

The exponents γ of the fitted power laws were obtained from Mishev et al. (2018). For the determination of the γ values, Mishev (2018) considered NM stations with cutoff rigidities ranging from zero GV (Terre Adelie, TERA) to 8.53 GV (Athens, ATHN), thus covering practically the entire energy spectrum. The γ-values for some specific time intervals taken from MIshev et al. (2018) are presented in Table 2.

September 10, 2017 Time Interval hh:mm - hh:mm	Power-law γ values	Rate of spectrum steepening δγ
16:15-16:20	4.8	0.8
16:30-16:35	5.5	0.7
16:45-16:50	5.6	0.3
17:00-17.05	6.4	0.2
17.30-17:35	7.1	0.0
18:00-18:05	7.4	0.0
18:30-18:35	7.3	0.0
19:00-19:05	7.6	0.0
20:00-20:05	7.7	0.0
21:00-21:05	7.9	0.0
22:00-22:05	8.1	0.0

Table 2 : Power-law γ values of GLE72 on September 10, 2017 obtained from Mishev et al. (2018).

2.2 Satellite data

For the evaluation of the results data from the GOES 13 satellite were used for direct comparison between the calculated and the recorded values of normalized proton intensity. The data were downloaded from (https://satdat.ngdc.noaa.gov/sem/goes/data/avg/2017/09/goes13/csv/). More specifically the P5, P6, P7, P8, P9, P10 and P11 channels were considered, corresponding to proton flux of 46 MeV, 104 MeV, 148 MeV (Sandberg et al., 2011), 375 MeV, 465 MeV, 605 MeV in units of p/cm^2 s sr MeV and integral proton flux of >700MeV (processed as differential flux at 1000 MeV in units p/cm^2 s sr MeV),

respectively. The time profile of the proton fluxes mentioned above, are presented in Figure 2.

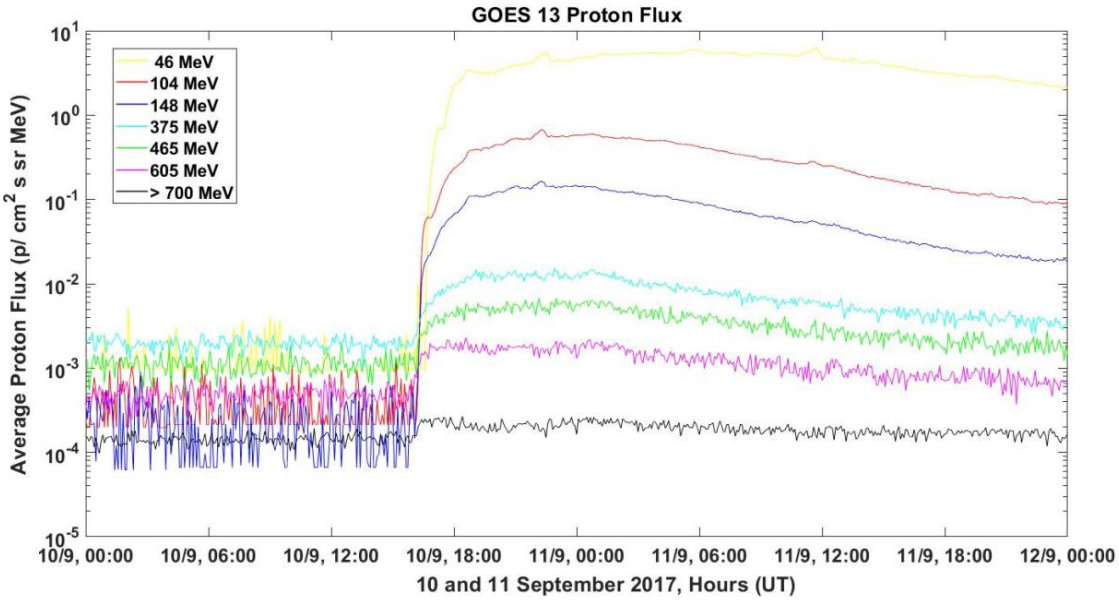

Fig. 2: Time profile of the average proton flux at energy channel of 46, 104, 148, 375, 465, 605 and >700 MeV, as recorded by the GOES 13 satellite during 10 and 11 September, 2017.

For the remainder of this work we will only use the data values from the energy channel of protons with E >700 MeV (black line) for comparison with the calculated proton normalized intensity. This channel is measured by the High-Energy Proton and Alpha Detector (HEPAD) (Rinehart, 1978; Raukunen et al., 2020) onboard GOES 13.

3. Application of the coupling function

The starting point of our calculations is the relation between secondary and primary Cosmic Ray intensities (Clem and Dorman, 2000):

$$\frac{\delta N(t)}{N} = \int_{E_{cut}}^{\infty} W(E) \frac{\delta D(E,t)}{D} dE \qquad (2)$$

where

$$W(E) = 1.65 * 10^{-2} \frac{1}{E^3} \left[\ln\left(\frac{E}{E_{cut}} \right) \right]^2 \left[\frac{5}{1 - 0.095 \ln\left(\frac{E}{E_{cut}} \right)} \right]^2 \quad (3)$$

is the theoretically derived coupling function (Xapanteris et al., 2021; 2020), δN(t)/N is the secondary CR intensity spectrum as a function of time provided by NMDB data and δD(E,t)/D is the primary CR intensity spectrum as a function of both energy and time, which will be determined.

Following the same assumption as in Xaplanteris et al., 2020, we express the primary CR spectrum, which is a function of two parameters, energy and time, as a separable product of two factors, one energy-dependent and another time-dependent:

$$\frac{\delta D(E,t)}{D} = \frac{\delta D_I(t)}{D} \frac{\delta D_{II}(E)}{D} \quad (4)$$

We also assume that the energy dependent part of the primary spectrum $\delta D_{II}(E)/D$ has a power law form (Mishev et al., 2018) :

$$\frac{\delta D_{II}(E)}{D} = \left(\frac{E}{E_{cut}} \right)^{-\gamma(t)} \quad (5)$$

where the values of the exponent γ for different time intervals are given in Table 2.

With the analytical assumptions discussed above, the primary cosmic ray spectrum as a function of time is determined by:

$$\frac{\delta D_I(t)}{D} = \frac{1}{I} F_{al} \frac{\delta N(t)}{N} \quad (6)$$

where :

$$I = \int_{E_{cut}}^{\infty} W(E) \left(\frac{E}{E_{cut}} \right)^{-\gamma} dE \quad (7)$$

and

$$F_{al}(H) = \frac{\int_{0}^{h_u} n_0 \exp\left(-\frac{mgh}{kT(h)}\right) dh}{\int_{H}^{h_u} n_0 \exp\left(-\frac{mgh}{kT(h)}\right) dh} \qquad (8)$$

is the altitude correction factor for each NM station.

Moreover, n_0 is the concentration of atmospheric particles at ground level, m is the (an average) mass of atmospheric particles, g is the gravitational acceleration, h is the altitude , measured from sea level upward, H the altitude of each NM station, k is the Boltzmann constant and T is the absolute temperature (K).

This correction factor has been deduced analytically in Xaplanteris et al. (2021) under the assumption that the concentration of atmospheric particles follows a Boltzmann distribution as a function of altitude (Seinfeld, 2006). In equation (8) H is the altitude of each NM station and h_u is the upper limit of the atmosphere for the geomagnetic coordinates of each NM station. In this work, h_u was taken as 8 km above sea level for all stations.

In Figure 3 we determine the primary CR intensity spectrum from each NM station along with the normalized proton flux for energy > 700 MeV as recorded by GOES 13 satellite for direct comparison.

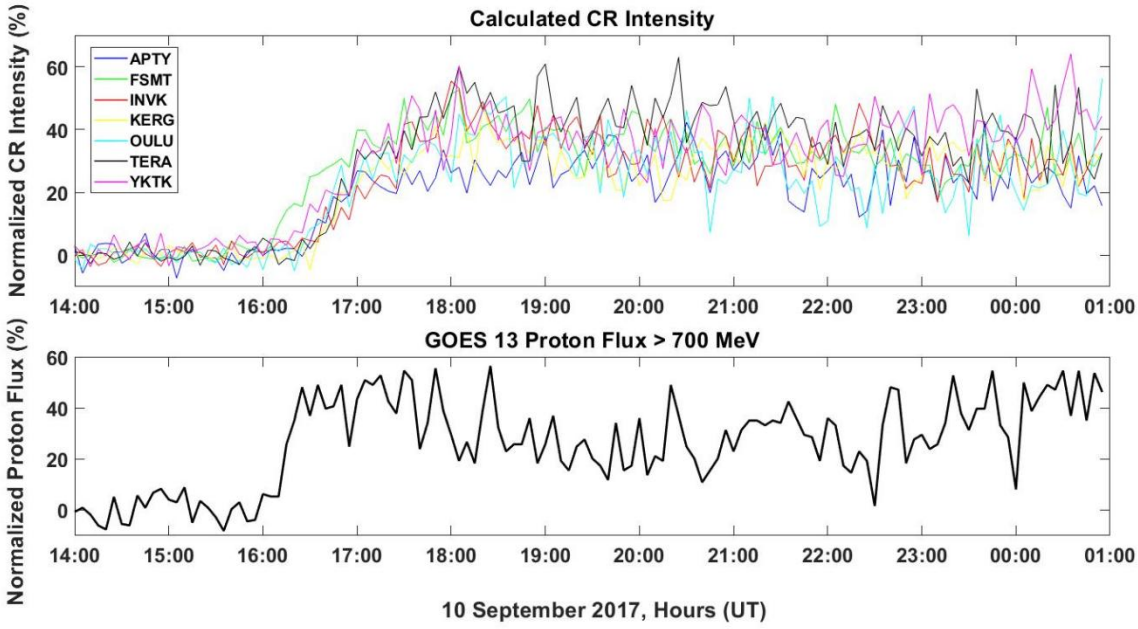

Fig. 3 : Time profile of the calculated normalized cosmic ray intensity increase for seven neutron monitor stations (upper panel) alongside the recorded normalized proton flux for energy >700 MeV from GOES 13 during September 10, 2017 (lower panel).

At this point we should mention that the lowest limit of integration in equations (2) and (7) was taken as E_{cut} = 1 GeV for all NM stations considered in our study. This choice was dictated by the fact that our theoretical coupling function holds for the condition E ≥ 1 GeV as discussed in Xaplanteris et al. (2021). This means that for every NM station we have omitted a contribution to the integral of the form:

$$I_1 = \int_{E_{cut}}^{1} W(E)\left(\frac{E}{E_{cut}}\right)^{-\gamma} dE \qquad (9)$$

where E_{cut} is the cutoff energy value of each station (Table 1).

We thus implicitly argue that integral I_1 in Equation (9) is negligible compared to the integral I of equation (7). More specifically, the value of integral I_1 when computed using either Dorman's

$$W_D(R) = 9.879 * R^{-1.9615} \exp(-10.275 * R^{-0.9615}) \qquad (10)$$

or Caballero-Lopez

$$W_{CL-M}(R) = 4.37 * 10^{-4} (0.089^{0.9} + R^{0.9})^{-67.28} R^{61.3} \qquad (11)$$

coupling function (Caballero-Lopez, 2016) is at least three orders of magnitude smaller than the one of the integral in the higher energy region, E ≥ 1 GeV. Therefore, our analytical approximation of imposing E_{cut} ≥ 1 GeV can be considered appropriate.

It should be noted that the two coupling functions of eqs. (10), (11) used for the determination of the I_1 integral contribution (eq. 9) are functions of the rigidity R. For the conversion from rigidity to energy we used the following relation :

$$\mathrm{R} = \frac{A}{Z}\sqrt{E^2 + 2EM_0} \qquad (12)$$

where R is the rigidity, A is the mass number, Z is the charge, E is the energy per nucleon, M_0 is the rest mass per nucleon. For the case of protons under study here, A = Z = 1 and M_0 = 1 GeV.

In Figure 4 we present the direct comparison between the time profiles of the mean value of the calculated normalized proton intensity for energy E ≥ 1 GeV from our selected seven NM stations with the normalized proton flux recorded by GOES 13 for energy E ≥ 700 MeV for GLE 72. We reiterate that for the normalization of both sets of results the time interval of half an hour before the start of the increase has been considered (i.e., 14:00-14:30 UT).

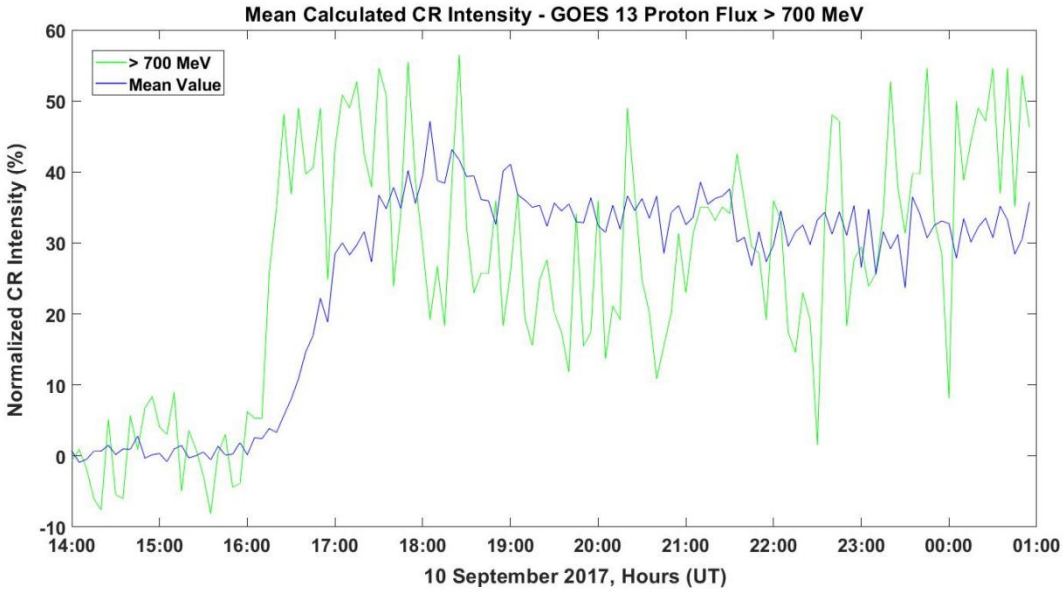

Fig. 4 : Time profile of the mean calculated normalized cosmic ray intensity increase from seven neutron monitor stations along with the recorded normalized proton flux for energy >700 MeV from GOES 13 on September 10, 2017.

Figure 4 shows that the time profile of the normalized proton flux with energy > 700 MeV recorded by GOES 13 is in qualitative agreement with the corresponding mean calculated normalized proton intensity from the NM stations on the ground.

For a quantitative comparison and evaluation between the two sets of results we present in Figure 5 the scatter plot between the mean value of the calculated normalized intensity increases and the corresponding normalized proton flux increase recorded by GOES 13 satellite for E > 700 MeV.

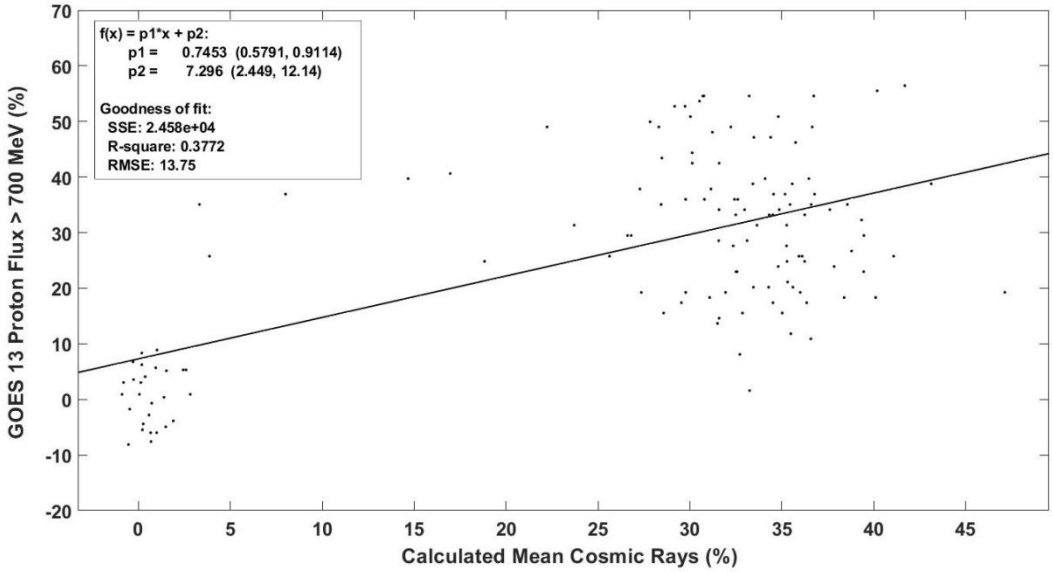

Fig. 5: Scatter plot of the normalized proton flux for energy E > 700 MeV detected by the GOES satellite and the mean value of calculated primary CR intensity from seven NM stations using the coupling function of equation (3), for the GLE 72.

As we can see from Figure 4, the two sets of results are in good agreement meaning that the onset time of the GLE 72 event is similar for both, around 16:18 UT, with the GOES 13 data showing a more impulsive start of the event a few minutes earlier from the NM data.
Moreover the maximum value of the mean normalized relative increase from all NM stations ($\approx$45%) is relatively close with the maximum value of the corresponding increase of the satellite data ($\approx$55%). The discrepancy between the maximum amplitude values in the two sets of data can be attributed to the fact that the atmosphere works as a protective shield and reduces the intensity and amplitude of the event unlike deep space.

The two sets of data in Figure 5 are in good agreement with each other as can be seen from the significant Pearson correlation coefficient r=0.62 and a goodness of fit R^2 = 0.3772. The slope of the least squares best-fit is p1 = 0.75 (± 0.17). The linear fit shown in Figure 5 holds at a confidence level exceeding 99%

4. Summary and Conclusions

In this work we applied the theoretically derived coupling function of Xaplanteris et al. (2020) to the case of GLE events for the first time. The computation of this particular version of the coupling function relies on fundamental QFT calculations and tools with the inclusion of an analytically derived altitude correction factor. Until now it has been applied to the case of Forbush decreases (Xaplanteris et al., 2020; 2021) yielding satisfactory results when compared to the corresponding ones using the GSM technique (Belov et al., 2018).

In order to apply the coupling function to a GLE event for the first time, ground based measurements recorded by seven NM stations having low cutoff rigidities (below the energy requirement of 1 GeV of the coupling function) were used. By setting the lower limit of the integral in equation (7) equal to 1 GeV we calculate the proton spectrum. The contribution of the energy spectrum from cutoff energy value of each station up to 1 GeV, as given by equation (9), is found to be negligible, considered by means of two widely known coupling functions, those of Dorman (2000) and Caballero-Lopez (2016).

After calculating the normalized time profile of proton intensity resulted by the coupling function, we compared it to the normalized proton flux data with energy > 700 MeV, as recorded from the GOES 13 satellite. Even though the two data sets refer to close but not identical energy regions, they follow in general a similar time evolution as can be seen from figure 4, with the GOES 13 values starting a few minutes earlier that the calculated NM values. Moreover, they present a slope value of their linear fit equal to 0.75 ($\pm$0.17) and a Pearson correlation coefficient r equal to 0.62 (see figure 5). From the above it can be concluded that our calculated values

are in good agreement with the detected ones. However, a small deviation in the maximum normalized values between the >700 MeV and >1 GeV appears. This is mainly due to the fact that the atmosphere shields the Earth from the entirety of the event, thus we compute reduced amplitude values of the GLE 72 compared to the one from direct GOES 13 data.

In conclusion, in this study we have demonstrated that the coupling function used herein is applicable to both Forbush decreases (Xaplanteris et al., 2021) and to GLE events. The advantage of the analytical approach that was followed is that it can describe adequately events in which there is a variation (either increase or decrease) in the intensity of the particles involved. So, this procedure provides a key tool for the study of cosmic ray events regardless of the different physical mechanisms that cause them.

A potential extension of this study could be the extrapolation of this analytical coupling function to energies lower than 1 GeV. This extrapolation will render our function applicable to the data of all NM Network stations, without any energy limitations due to low cutoff rigidities. This extrapolation might be obtained by means of a parameterization technique. It would be worthwhile to apply our method to the recently detected GLE 73 on October 28, 2021 which is one of our plans in order to further increase the validity of the analytical procedure we followed.

Acknowledgments: We are grateful to our collaborators of the Neutron Monitor stations for kindly providing the cosmic ray data used in this work in the frame of the high resolution real time Neutron Monitor Database (NMDB), funded under the European Union's FP7 Program (contract no. 213007). Athens Neutron Monitor Station (A.Ne.Mo.S.) is supported by the Special Research Account of the National and Kapodistrian University of Athens. J. V. Rodriguez was supported by the NOAA Cooperative Agreement with CIRES, NA17OAR4320101.

Conflict of Interests: The authors declare that they have no conflict of interest.

References

Agostinelli, S., Allison, J., Amako, K., Apostolakis, J., Araujo, H., Arce, P., et al.: 2003, Geant4-a simulation toolkit. *Nucl. Instr. Meth. Phys. Res. A,* **506,** 250. https://doi.org/10.1016/S0168-9002(03)01368-8.

Andriopoulou, M., Mavromichalaki, H., Plainaki, C., Belov, A., Eroshenko, E.: 2011, Intense Ground-Level Enhancements of Solar Cosmic Rays During the Last Solar Cycles. *Solar Phys*. **269,** 155. DOI 10.1007/s11207-010-9678-1.

Balabin, Y., Gvozdevsky, B., Germanenko, A., Maurchev, E.: 2018, GLE events in 24th solar cycle. *E3S Web of Conferences* **62**, 01006. https://doi.org/10.1051/e3sconf/20186201006.

Belov, A., Eroschenko, E., Yanke, V., Oleneva, V., Abunin, A., Abunina, M., Papaioannou, A., Mavromichalaki, H.: 2018, The global survey method applied to ground-level cosmic ray measurements. *Solar Phys.* **293**, 68. https://doi.org/10.1007/s11207-018- 1277-6.

Belov, A.V., Eroshenko, E.A., Kryakunova, O.N. et al.: 2010, Ground level enhancements of solar cosmic rays during the last three solar cycles. *Geomagn. Aeron*. **50,** 21. https://doi.org/10.1134/S0016793210010032.

Bütikofer, R. and Flückiger, E. O. for the NMDB Team: 2009, Near real-time determination of ionization and radiation dose rates induced by cosmic rays in the earth's atmosphere - A NMDB application. *Proc. 31st ICRC*, Lodz.

Caballero-Lopez, R.A.: 2016, An estimation of the yield and response functions for the mini neutron monitor. *J. Geophys. Res.* **121,** 7461–7469. doi:10.1002/2016JA022690.

Caballero-Lopez, R., Moraal, H.: 2012, Cosmic-ray yield and response functions in the atmosphere. *J. Geophys. Res.* **117,** A 12103. https://doi.org/10.1029/2012JA017794.

Clem, J.M., Dorman, L.I.: 2000, Neutron monitor response functions. *Space Sci. Rev*. **93**, 335. https://doi.org/10.1023/A:1026508915269.

Copeland, K., Matthiä, D. and Meier, M. M.: 2018, Solar cosmic ray dose rate assessments during GLE 72 using MIRA and PANDOCA. *Space Weather*, 16. https://doi.org/10.1029/2018SW001917.

Desorgher, L., Flückiger, E. O., Gurtner, M., Moser, M.R., Bütikofer, R.: 2005, Atmocosmics: a Geant 4 Code for Computing the Interaction of Cosmic Rays with the Earth's Atmosphere. *Intern. J. Modern Phys. A*, **20,** 6802. https://doi.org/ 10.1142/S0217751X0503013.

Dorman, L.: 2004, Cosmic Rays in the Earth's Atmosphere and Underground, Kluwer, Dordrecht. DOI: 1-4020- 2071-6.

Dorman, L.I., Villoresi, G., Iucci, N., et al.: 2000, Cosmic ray survey to Antarctica and coupling functions for neutron component near solar minimum (1996-1997), Geomagnetic effects and coupling functions. *J. Geophys. Res.* ***105****, A9, 21047.* https://doi.org/10.1029/2000JA900051.

Dorman, L.I.: 1974, Cosmic Rays Variations and Space Explorations. *North-Holland Publishing Company*.

Forbush, S.: 1946, Three unusual cosmic-ray increases possibly due to charged particles from the Sun. *Phys. Rev*. **70**, 771. https://doi.org/10.1103/PhysRev.70.771.

Golubenko, K., Rozanov, E., Mironova, I., Karagodin, A., Usoskin, I.: 2020, Natural sources of ionization and their impact on atmospheric electricity. *Geophys. Res. Lett*. 47:e2020GL088619. doi: 10.1029/2020GL088619.

Griffiths, D. Introduction to Elementary particles: 2008, Weinheim. Wiley-VCH, Germany, 9783527406012.

Kataoka, R., Sato, T., Miyake, S., Shiota, D., Kubo, Y.: 2018, Radiation dose nowcast for the ground level enhancement on 10–11 September. *Space Weather*, **16**, 917–923. https://doi.org/10.1029/2018SW001874.

Kurt, V., Belov, A., Kudela, K., Mavromichalaki, H., Kashapova, L. K. , Yushkov, B., Sgouropoulos C.: 2019, Onset Time of the GLE 72 Observed at Neutron Monitors and its Relation to Electromagnetic Emissions. *Solar Phys*. **294**, 22. https://doi.org/10.1007/s11207-019-1407-9

Maurin, D., Cheminet, A., Derome, L., Ghelfi, A., Hubert, G.: 2015, Neutron monitors and muon detectors for solar modulation studies: Interstellar flux, yield function, and assessment of critical parameters in count rate calculations. *Adv. Space Res*. **55**, 1, 363. DOI: 10.1016/j.asr.2014.06.021.

Mavromichalaki, H., Gerontidou, M., Paschalis, P., Paouris, E., Tezari, A., Sgouropoulos, C., Crosby, N., Dierckxsens, M.: 2018, Real-Time Detection of the Ground Level Enhancement on 10 September 2017 by A.Ne.Mo.S.: System Report. *Space Weather* **16,** 11. https://doi.org/10.1029/2018SW001992.

Mavromichalaki, H., Papaioannou, A., Plainaki, C., Sarlanis, C., Souvatzoglou, G., Gerontidou, M., Papailiou, M., Eroshenko, E., Belov, A., Yanke, V., Flückiger, E.O., Bütikofer, R., et al.: 2011, Applications and usage of the real – time neutron monitor Database. *Adv. Space Res.* **47**, 2210. DOI: 10.1016/j.asr.2010.02.019.

Mishev, A., Usoskin, I.G., Raukunen, O. et al.: 2018, First Analysis of Ground-Level Enhancement (GLE) 72 on 10 September 2017: Spectral and Anisotropy Characteristics. *Solar Phys.* **293**, 136. https://doi.org/10.1007/s11207-018-1354-x

Mishev, A. L., Usoskin, I.G.: 2018, Assessment of the radiation environment at commercial jet-flight altitudes during GLE 72 on 10 September 2017 using neutron monitor data. *Space Weather*, **16**, 1921. https://doi.org/10.1029/2018SW001946.

Peskin, M.E., Schroeder, D.V.: 1995, An introduction to Quantum Field Theory. Perseus Books.

Raukunen, O., Paassilta, M., Vainio, R., Rodriguez, J.V., Eronen, T., Crosby, N., Dierckxsens, M., Jiggens, P., Heynderickx, D. and Sandberg, I.: 2020, Very high energy proton peak flux model. *J. Space Weather and Space Climate*, ***10*****,** 24, https://doi.org/10.1051/swsc/2020024

Rinehart, M. C.: 1978, Cerenkov counter for spacecraft application. *Nuclear Instruments and Methods* **154,** 303.

Sandberg, I., Jiggens, P., Heynderickx, D., Daglis, I. A.: 2014, Cross calibration of NOAA GOES solar proton detectors using corrected NASA IMP-8/GME data, *Geophys. Res. Lett., 41, 4435.* doi:10.1002/2014GL060469.

Seinfeld, J.H., Pandis, S.: 2006, Atmospheric Chemistry and Physics: From Air Pollution to Climate Change. John Wiley & Sons. ISBN 1118947401.

Shea, M., Smart, D.: 2000, Cosmic ray Implications for Human Health. *Space Sci. Rev*. **93**, 187. https://doi.org/10.1023/A:1026544528473.

Simpson, J.A.: 2000, The Cosmic Ray Nucleonic Component: the Invention and Scientific Uses of the Neutron Monitor. *Space Sci. Rev*. **93,** 11. https://doi.org/10.1023/A:1026567706183.

Souvatzoglou, G., Papaioannou, A., Mavromichalaki, H., Dimitroulakos, J., Sarlanis, C.: 2014, Optimizing the real-time ground level enhancement alert system based on neutron monitor measurements: Introducing GLE Alert Plus. *Space Weather* **12**, 633. https://doi.org/10.1002/2014SW001102

Srednicki, M.: 2007, Quantum Field Theory. Cambridge University Press. https://doi.org/ 10.1017/CBO9780511813917.

Tezari, A., Paschalis, P., Mavromichalaki, H., Karaiskos, P., Crosby, N., Dierckxsens, M.: 2020, Assessing Radiation Exposure inside the Earth's Atmosphere. Radiation Prot. Dos. **190**, 4. https://doi.org/10.1093/rpd/ncaa112.

Usoskin, I., Koldobskiy, S., Kovaltsov, G. A., Gil, A., Usoskina, I., Willamo, T., Ibragimov , A.: 2020, Revised GLE database: Fluences of solar energetic particles as measured by the neutron-monitor network since 1956. *A&A*, **640**, A17. https://doi.org/10.1051/0004-6361/202038272.

Velinov, P. I. Y., Asenovski, S., Mateev, L.: 2013, Numerical calculation of cosmic ray ionization rate profiles in the middle atmosphere and lower ionosphere with relation to characteristic energy intervals. Acta Geophysica **61**, 494. DOI: 10.2478/s11600-012-0084-y

Weinberg, S.: 1995, The Quantum Theory of Fields Vol. I. Cambridge University Press.

Xaplanteris, L., Livada, M., Mavromichalaki, H., Dorman, L., Georgoulis, M. K., Sarris, T. E.: 2021, Improved Approach in the Coupling Function Between Primary and Ground Level Cosmic Ray Particles Based on Neutron Monitor Data. *Solar Phys*. **296**, 91. https://doi.org/10.1007/s11207-021-01836-y

Xaplanteris, L., Livada, M., Mavromichalaki, H., Dorman, L.I.: 2020, A new approximate coupling function: The case of Forbush decreases. *New Astronomy* **82,** 101453. https://doi.org/10.1016/j.newast.2020.101453.